AD-A080 534 OKLAHOMA UNIV NORMAN SCHOOL OF AEROSPACE MECHANICAL --ETC F/G 20/11
EFFECTS OF SHEAR DEFORMATION AND ANISOTROPY ON THE THERMAL BEND--ETC(U)
DEC 79 J N REDDY, Y S HSU N00014-78-C-0647
UNCLASSIFIED OU-AMNE-79-20 NL

1 OF 1
AD
A080534

END
DATE
FILMED
3-80
DDC

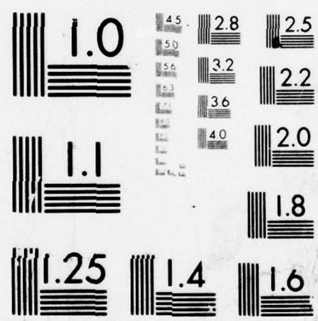

MICROCOPY RESOLUTION TEST CHART
NATIONAL BUREAU OF STANDARDS-1963-A

Department of the Navy
OFFICE OF NAVAL RESEARCH
Structural Mechanics Program
Arlington, Virginia 22217

15 Contract N00014-78-C-0647
Project NR 064-609
9 Technical Report No. 9

Report OU-AMNE-79-20, TR-9 14

6 EFFECTS OF SHEAR DEFORMATION AND ANISOTROPY ON THE THERMAL BENDING OF LAYERED COMPOSITE PLATES.

by

10 J. N. Reddy [redacted] Y. S. Hsu

11 Dec[redacted]79

12 27

School of Aerospace, Mechanical and Nuclear Engineering
University of Oklahoma
Norman, Oklahoma 73019

EFFECTS OF SHEAR DEFORMATION AND ANISOTROPY ON THE THERMAL BENDING OF LAYERED COMPOSITE PLATES

J. N. Reddy and Y. S. Hsu
School of Aerospace, Mechanical and Nuclear Engineering
University of Oklahoma, Norman, OK 73019

A finite-element formulation of equations governing layered anisotropic composite plates subjected to thermal and mechanical loadings is presented. An exact closed-form solution is also presented for simply supported rectangular cross-ply laminated plates under sinusoidal loading to validate the finite element developed herein. The finite-element results are in good agreement with the closed-form results and with the results of others. Material properties typical of advanced fiber-reinforced composites are used to show the parametric effects of plate aspect ratio, side-to-thickness ratio, orientation of layers, and edge conditions on the deflections and stresses.

INTRODUCTION

With the increased use of fiber-reinforced composites in aerospace and mechanical engineering structures, studies involving the thermomechanical behavior of composite-material plates and shells are receiving greater attention. Most of the previous research in the field of composites deals with isothermal problems. However, use of composites in environments with large temperature changes (e.g., space shuttle) requires the knowledge of thermally induced deflections and stresses. Further, thermal stresses are also induced during the fabrication of composite materials.

The problem of thermal bending of anisotropic plates was studied first by Pell [1], who derived the equations governing the transverse deflection of a thin plate. Generalization of Pell's work to heterogeneous plates subjected to arbitrary three-dimensional temperature distribution is due to

Stavsky [2]. Recent studies in the analysis of plates laminated of fiber-reinforced materials indicate that the thickness effect (i.e. shear deformation) on the behavior of the plate is more pronounced than in isotropic plates [3]. The shear deformation theory that has been proven to be adequate in predicting the overall response of laminated anisotropic plates is due to Yang, Norris and Stavsky [4]. Based on the Yang-Norris-Stavsky (YNS) theory, Reddy [5,6] developed a finite-element model that is algebraically simpler than previously developed finite elements [7-10], and yet possesses competitive accuracy.

The present investigation is concerned with the application of the penalty finite element [6] to the thermal stress analysis of layered anisotropic composite plates. To illustrate the accuracy of the present element, closed-form solutions are also presented for the equations governing (i.e., the YNS theory) simply supported, rectangular, cross-ply plates under sinusoidal mechanical and/or thermal loadings. Finite-element solutions are presented to show the effects of variations in geometry, lamination parameters, boundary conditions, and loading on the shear deformation and thermal response of statically loaded layered anisotropic composite plates.

GOVERNING EQUATIONS

Consider a plate of constant thickness t composed of a finite number of anisotropic layers with arbitrary orientations. The coordinate system is such that the middle plane of the plate coincides with the x-y plane, and the z-axis is normal to the middle plane, $\mathbb{R}$.

The displacement field in the YNS theory is assumed to be of the form

$$
\begin{aligned}
u &= u_0(x,y) + z\psi_x(x,y) \\
v &= v_0(x,y) + z\psi_y(x,y) \\
w &= w(x,y)
\end{aligned}
\qquad (1)
$$

where u, v, and w are the displacements along x, y, and z directions, respectively, u_o and v_o are the in-plane displacements of the mid-plane, and ψ_x and ψ_y are the shear rotations.

The equilibrium equations associated with the YNS theory are

$$N_{1,x} + N_{6,y} = p_1 \ , \ N_{6,x} + N_{2,y} = p_2 \ , \ Q_{1,x} + Q_{2,y} = -q$$
$$M_{1,x} + M_{6,y} - Q_1 = 0 \ , \ M_{6,x} + M_{2,y} - Q_2 = 0 \tag{2}$$

where $N_{i,x} = \partial N_i/\partial x$ etc., p_1 and p_2 are the in-plane distributed forces, q is the transversely distributed load, and N_i, Q_i and M_i are the stress and moment resultants defined by

$$(N_i, M_i) = \int_{-t/2}^{t/2} (1,z)\sigma_i \, dz \ , \ (Q_1, Q_2) = \int_{-t/2}^{t/2} (\sigma_{xz}, \sigma_{yz}) \, dz \tag{3}$$

Here $\sigma_i (i=1,2,6)$ denote the in-plane stress components ($\sigma_1 = \sigma_x$, $\sigma_2 = \sigma_y$, $\sigma_6 = \sigma_{xy}$).

Assuming monoclinic behavior (i.e., one plane of elastic symmetry) for each layer, the constitutive equations for an arbitrarily laminated plate are

$$\begin{Bmatrix} N_1 \\ N_2 \\ N_6 \\ Q_1 \\ Q_2 \\ M_1 \\ M_2 \\ M_6 \end{Bmatrix} = \begin{bmatrix} A_{11} & A_{12} & A_{16} & 0 & 0 & B_{11} & B_{12} & B_{16} \\ A_{12} & A_{22} & A_{26} & 0 & 0 & B_{12} & B_{22} & B_{26} \\ A_{16} & A_{26} & A_{66} & 0 & 0 & B_{16} & B_{26} & B_{66} \\ 0 & 0 & 0 & A_{44} & A_{45} & 0 & 0 & 0 \\ 0 & 0 & 0 & A_{45} & A_{55} & 0 & 0 & 0 \\ B_{11} & B_{12} & B_{16} & 0 & 0 & D_{11} & D_{12} & D_{16} \\ B_{12} & B_{22} & B_{26} & 0 & 0 & D_{12} & D_{22} & D_{26} \\ B_{16} & B_{26} & B_{66} & 0 & 0 & D_{16} & D_{26} & D_{66} \end{bmatrix} \begin{Bmatrix} u_{o,x} \\ v_{o,y} \\ u_{o,y}+v_{o,x} \\ w_{,x}+\psi_x \\ w_{,y}+\psi_y \\ \psi_{x,x} \\ \psi_{y,y} \\ \psi_{x,y}+\psi_{y,x} \end{Bmatrix} - \begin{Bmatrix} N_1^T \\ N_2^T \\ N_6^T \\ 0 \\ 0 \\ M_1^T \\ M_2^T \\ M_6^T \end{Bmatrix}$$

The plate stiffnesses A_{ij}, B_{ij}, and D_{ij} are given by

$$(A_{ij},B_{ij},D_{ij}) = \sum_m \int_{z_m}^{z_{m+1}} Q_{ij}^{(m)}(1,z,z^2)\,dz\ ,\ (i,j = 1,2,6)$$

$$A_{ij} = \sum_m \int_{z_m}^{z_{m+1}} k_\alpha k_\beta Q_{ij}^{(m)}\,dz\ ,\ (\alpha = 6-i,\ \beta = 6-j;\ i,j = 4,5) \tag{5}$$

where $Q_{ij}^{(m)}$ are the stiffness coefficients of the m-th layer in the plate coordinates, and z_m is the distance from the mid-plane to the lower surface of the m-th layer. The stress and moment resultants, N_i^T and M_i^T, due to thermal loading are defined by

$$(N_i^T,M_i^T) = \sum_m \int_{z_m}^{z_{m+1}} \sum_j Q_{ij}^{(m)}\ \alpha_j(T_o,zT_1)\,dz\ ,\ (i,j = 1,2,6) \tag{6}$$

where α_i are the thermal coefficients of expansion in the plate coordinates, and T is the temperature change from a reference state,

$$T(x,y,z) = T_o(x,y) + zT_1(x,y) \tag{7}$$

Note that the temperature variation through the thickness is assumed to be linear, consistent with the plate theory.

Substituting Eq. (4) into Eq. (2), we obtain the following operator equation,

$$[L]\{\delta\} = \{f\} \tag{8}$$

where $\{\delta\} = \{u_o,v_o,w,\psi_x,\psi_y\}^T$, [L] is the (symmetric) matrix of differential operators,

$L_{11} = A_{11}d_{11} + 2A_{16}d_{12} + A_{66}d_{22}$

$L_{12} = (A_{12}+A_{66})d_{12} + A_{16}d_{11} + A_{26}d_{22}\ ,\ L_{13} = 0\ ,$

$L_{14} = B_{11}d_{11} + 2B_{16}d_{12} + B_{66}d_{22}$

$L_{15} = (B_{12}+B_{66})d_{12} + B_{16}d_{11} + B_{26}d_{22} = L_{24}\ ,$

$L_{22} = 2A_{26}d_{12} + A_{22}d_{22} + A_{66}d_{11}\ ,\ L_{23} = 0\ ,$

$L_{25} = 2B_{26}d_{12} + B_{22}d_{22} + B_{66}d_{11}$

$$L_{33} = -A_{44}d_{11}-2A_{45}d_{12}-A_{55}d_{22},\ L_{34} = -A_{44}d_{1}-A_{45}d_{2}$$

$$L_{35} = -A_{45}d_{1}-A_{55}d_{2},\ L_{44} = D_{11}d_{11}+2D_{16}d_{12}+D_{66}d_{22}-A_{44}$$

$$L_{45} = (D_{12}+D_{66})d_{12}+D_{16}d_{11}+D_{26}d_{22}-A_{45},\ L_{55} = 2D_{26}d_{12}+D_{22}d_{22}+D_{66}d_{11} \tag{9}$$

and the components of the generalized force vector, $\{f\}$, are given by

$$\begin{aligned} f_1 &= N^T_{1,x} + N^T_{6,y} + P_1\ ,\ f_2 = N^T_{6,x} + N^T_{2,y} + P_2 \\ f_3 &= q\ ,\ f_4 = M^T_{1,x} + M^T_{6,y}\ ,\ f_5 = M^T_{6,x} + M_{2,y} \end{aligned} \tag{10}$$

In Eq. (9), d_{ij} denote the differential operators

$$d_{ij} = \frac{\partial^2}{\partial x_i \partial x_j}\ ,\ d_i = d_{io} = \frac{\partial}{\partial x_i}\ ,\ (i,j = 0,1,2)$$

EXACT CLOSED-FORM SOLUTION

The boundary-value problem associated with the equilibrium of layered anisotropic composite plates involves solving the operator equation (8) subjected to a given set of boundary conditions. It is not possible to construct exact solutions to Eq. (8) when the plate is of arbitrary geometry, constructed of arbitrarily-oriented layers, and subjected to an arbitrary loading or boundary conditions. However, an exact closed-form solution to Eq. (8) can be constructed when the plate is of rectangular geometry with the following edge conditions, loading, and plate construction.

<u>Boundary conditions</u> (freely supported)

$$\begin{aligned} &u(x,0) = u(x,b) = 0,\ N_2(x,0) = N_2(x,b) = 0 \\ &v(0,y) = v(a,y) = 0,\ N_1(0,y) = N_1(a,y) = 0 \\ &w(x,0) = w(x,b) = w(0,y) = w(a,y) = 0 \\ &\psi_x(x,0) = \psi_x(x,b) = 0,\ M_2(x,0) = M_2(x,b) = 0 \\ &\psi_y(0,y) = \psi_y(a,y) = 0,\ M_1(0,y) = M_1(a,y) = 0 \end{aligned} \tag{11}$$

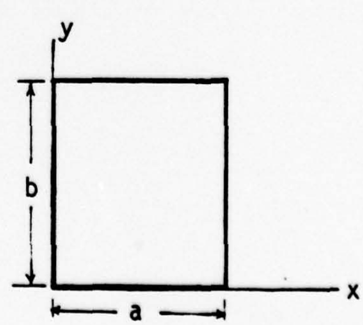

<u>Loading</u> (sinusoidal)

$$q=q_o^{mn}\sin\alpha x\sin\beta y,\; T_o=\bar{T}_o^{mn}\sin\alpha x\sin\beta y,\; T_1=\bar{T}_1^{mn}\sin\alpha x\sin\beta y$$
$$P_1=\bar{P}_1^{mn}\sin\alpha x\cos\beta y\;,\; P_2=\bar{P}_2^{mn}\cos\alpha x\sin\beta y\;,\;\alpha=m\pi/a\;,\;\beta=n\pi/b \tag{12}$$

and m and n are integers.

<u>Plate construction</u> (cross-ply, i.e., θ_m should be either 0° or 90°)

$$A_{16}=A_{26}=A_{45}=0\;,\; B_{16}=B_{26}=0\;,\; D_{16}=D_{26}=0\;,\;\alpha_6=0 \tag{13}$$

Under these specific conditions, the solution $(u_o, v_o, w, \psi_x, \psi_y)$ to Eq. (8) is of the form,

$$u_o=U_{mn}\cos\alpha x\sin\beta y\;,\; v_o=V_{mn}\sin\alpha x\cos\beta y$$
$$w=W_{mn}\sin\alpha x\sin\beta y \tag{14}$$
$$\psi_x=X_{mn}\cos\alpha x\sin\beta y\;,\;\psi_y=Y_{mn}\sin\alpha x\cos\beta y$$

where U_{mn}, V_{mn}, etc. are parameters to be determined subjected to the condition that the solution in Eq. (14) satisfies the operator equation (8). Substituting Eq. (14) into Eq. (8), we get

$$[C]\{\Delta\}=\{F\} \tag{15}$$

where

$$\{\Delta\}=\{U_{mn}, V_{mn}, W_{mn}, X_{mn}, Y_{mn}\}^T,\; \{F\}=\{\bar{F}_1^{mn},\bar{F}_2^{mn},\bar{F}_3^{mn},\bar{F}_4^{mn},\bar{F}_5^{mn}\}^T$$

and the elements of the coefficient matrix, [C], are given by

$$\begin{aligned}
&C_{11}=-A_{11}\alpha^2-A_{66}\beta^2,\; C_{12}=-(A_{12}+A_{66})\alpha\beta\\
&C_{13}=0,\; C_{14}=-\alpha^2B_{11}-B_{66}\beta^2,\; C_{15}=-(B_{12}+B_{66})\alpha\beta\\
&C_{22}=-A_{22}\beta^2-A_{66}\alpha^2,\; C_{23}=0,\; C_{24}=C_{15}\;,\\
&C_{25}=-B_{22}\beta^2-A_{66}\alpha^2,\; C_{33}=-\alpha^2A_{55}-\beta^2A_{44}\\
&C_{34}=-\alpha A_{55},\; C_{35}=-\beta A_{44},\; C_{44}=-D_{11}\alpha^2-D_{66}\beta^2-A_{55}\\
&C_{45}=-(D_{12}+D_{66})\alpha\beta\;,\; C_{55}=-D_{66}\alpha^2-D_{22}\beta^2-A_{44}
\end{aligned} \tag{17}$$

Thus, for a given $\alpha = m\pi/a$, $\beta = n\pi/b$, q_0, $\bar{F}_i^{mn}$ (see (10) and (12)), and cross-ply construction, one needs to solve the 5 by 5 matrix equation (15) for the vector $\{\Delta\}$ of amplitudes of the generalized displacements.

FINITE-ELEMENT FORMULATION

As pointed out in the previous section, exact solution to Eq. (8) can be obtained only under special conditions of geometry, edge conditions, loadings, and lamination. Here we present a simple finite-element formulation which does not have any limitations (except for those implied in the formulation of the governing equations).

Suppose that the region R is subdivided into a finite number N of subregions or finite elements, R_e (e = 1,2,...,N). Over each element the generalized displacements $(u_0, v_0, w, \psi_x, \psi_y)$ are interpolated according to

$$u_0 = \sum_i^r u_i\phi_i^1 \, , \quad v_0 = \sum_i^r v_i\phi_i^1 \, , \quad w = \sum_i^s w_i\phi_i^2 \, ,$$

$$\psi_x = \sum_i^p \psi_{xi}\phi_i^3 \, , \quad \psi_y = \sum_i^p \psi_{yi}\phi_i^3 \tag{18}$$

where ϕ_i^α (α = 1,2,3) is the interpolation function corresponding to the i-th node in the element. Note that the in-plane displacements, the transverse displacement, and the slope functions are approximated by different sets of interpolation functions. While this generality is included in the formulation (to indicate the fact that such independent approximations are possible), we dispense with it in the interest of simplicity when the element is actually programmed and take $\phi_i^1 = \phi_i^2 = \phi_i^3$ (r = s = p). Here r, s, and p denote the number of degrees of freedom per each variable. That is, the total number of degrees of freedom per element is 2r + s + 2p.

Substituting Eq. (18) into the Galerkin integrals associated with the operator equation (8), which must also hold in each element R_e,

$$\int_{R_e} ([L]\{\delta\} - \{f\})\{\phi\}\, dx\, dy = 0 \tag{19}$$

and using integration by parts once (to distribute the differentiation equally between the terms in each expression), we obtain

$$\begin{bmatrix} [K^{11}] & [K^{12}] & [0] & [K^{14}] & [K^{15}] \\ [K^{12}] & [K^{22}] & [0] & [K^{24}] & [K^{25}] \\ [0] & [0] & [K^{33}] & [K^{34}] & [K^{35}] \\ [K^{14}] & [K^{24}] & [K^{34}] & [K^{44}] & [K^{45}] \\ [K^{15}] & [K^{25}] & [K^{35}] & [K^{45}] & [K^{55}] \end{bmatrix}_e \begin{Bmatrix} \{u\} \\ \{v\} \\ \{w\} \\ \{\psi_x\} \\ \{\psi_y\} \end{Bmatrix}_e = \begin{Bmatrix} \{F^1\} \\ \{F^2\} \\ \{F^3\} \\ \{F^4\} \\ \{F^5\} \end{Bmatrix}_e \tag{20}$$

where the $\{u\}$, $\{v\}$, etc. denote the columns of the nodal values of u, v, respectively, and the elements $K_{ij}^{\alpha\beta}$ $(\alpha,\beta = 1,2,\ldots,5)$ of the stiffness matrix and F_i^{α} of the force vector are given by

$$K_{ij}^{11} = A_{11}G_{ij}^{x} + A_{16}(G_{ij}^{xy} + G_{ji}^{xy}) + A_{66}G_{ij}^{y}$$

$$K_{ij}^{12} = A_{12}G_{ij}^{xy} + A_{16}G_{ij}^{x} + A_{26}G_{ij}^{y} + A_{66}G_{ji}^{xy}$$

$$K_{ij}^{14} = B_{11}H_{ij}^{x} + B_{16}(H_{ij}^{xy} + H_{ji}^{xy}) + B_{66}H_{ij}^{y}$$

$$K_{ij}^{15} = B_{12}H_{ij}^{xy} + B_{16}H_{ij}^{x} + B_{26}H_{ij}^{y} + B_{66}H_{ji}^{xy}$$

$$K_{ij}^{22} = A_{26}(G_{ij}^{xy} + G_{ji}^{xy}) + A_{22}G_{ij}^{y} + A_{66}G_{ij}^{x}$$

$$K_{ij}^{24} = B_{16}H_{ij}^{x} + B_{66}H_{ij}^{xy} + B_{12}H_{ji}^{xy} + B_{26}H_{ij}^{y}$$

$$K_{ij}^{25} = B_{26}(H_{ij}^{xy} + H_{ji}^{xy}) + B_{66}H_{ij}^{x} + B_{22}H_{ij}^{y}$$

$$K^{33} = A_{44}S_{ij}^{x} + A_{45}(S_{ij}^{xy} + S_{ji}^{xy}) + A_{55}S_{ij}^{y}$$

$$K^{34} = A_{44}R_{ij}^{xo} + A_{45}R_{ij}^{yo}\,,\quad K_{ij}^{35} = A_{45}R_{ij}^{xo} + A_{55}R_{ij}^{yo}$$

$$K_{ij}^{44} = D_{11}T_{ij}^{x} + D_{16}(T_{ij}^{xy} + T_{ji}^{xy}) + D_{66}T_{ij}^{y} + A_{44}T_{ij}^{o}$$

$$K_{ij}^{55} = D_{26}(T_{ij}^{xy} + T_{ji}^{xy}) + D_{66}T_{ij}^{x} + D_{22}T_{ij}^{y} + A_{55}T_{ij}^{o} \tag{21}$$

$$F_i^{\alpha} = \int_{R_e} f_\alpha \phi_i^1 \, dx\, dy, \ (\alpha = 1,2;\ i = 1,2,\ldots,r)$$

$$F_i^{3} = \int_{R_e} q \phi_i^2 \, dx\, dy, \ (i = 1,2,\ldots,s)$$

$$F_i^{\alpha} = \int_{R_e} f_\alpha \phi_i^3 \, dx\, dy, \ (\alpha = 4,5;\ i = 1,2,\ldots,r) \tag{22}$$

where

$$G_{ij}^{\xi\eta} = \int_{R_e} \phi_{i,\xi}^1 \, \phi_{j,\eta}^1 \, dx\, dy\ ,\ (i,j = 1,2,\ldots,r)$$

$$H_{ij}^{\xi\eta} = \int_{R_e} \phi_{i,\xi}^1 \, \phi_{j,\eta}^3 \, dx\, dy\ ,\ (i = 1,2,\ldots,r;\ j = 1,2,\ldots,t)$$

$$S_{ij}^{\xi\eta} = \int_{R_e} \phi_{i,\xi}^2 \, \phi_{j,\eta}^2 \, dx\, dy\ ,\ (i,j = 1,2,\ldots,s)$$

$$R_{ij}^{\xi\eta} = \int_{R_e} \phi_{i,\xi}^2 \, \phi_{j,\eta}^3 \, dx\, dy\ ,\ (i = 1,2,\ldots,s;\ j = 1,2,\ldots,t)$$

$$T_{ij}^{\xi\eta} = \int_{R_e} \phi_{i,\xi}^3 \, \phi_{j,\eta}^3 \, dx\, dy\ ,\ (i.j = 1,2,\ldots,t)\ ,\ (\xi,\eta = 0,x,y) \tag{23}$$

and $G_{ij}^{xx} = G_{ij}^{x}$, etc. In the special case in which $\phi_i^1 = \phi_i^2 = \phi_i^3$, all of the matrices in Eq. (23) will coincide.

In the present study rectangular elements of the serendipity family are employed with the same interpolation for all of the variables. The resulting stifness matrices are 20 by 20 for 4-node element and 40 by 40 for the 8-node element. As pointed out in a recent study [6], the YNS theory can be derived from the corresponding classical thin plate theory by treating the slope-displacement relations

$$\frac{\partial w}{\partial x} = -\theta_x \, , \; \frac{\partial w}{\partial y} = -\theta_y \tag{24}$$

as constraints. Indeed, when the constraints in Eq. (24) are incorporated into the classical-thin plate theory by means of the penalty method, the resulting equations correspond to the YNS theory with the correspondence,

$$\theta_x \sim \psi_x \text{ and } \theta_y \sim \psi_y \tag{25}$$

It is now well-known that whenever the penalty method is used, the so-called reduced integration [11] must be used to evaluate the matrix coefficients in Eq. (21). That is, if the four-node rectangular element is used, the 1 x 1 Gauss rule must be used in place of the standard 2 x 2 Gauss rule to numerically evaluate the coefficients K_{ij}. For more details on the effect of reduced integration on the solution accuracy, one can consult [12,13].

NUMERICAL RESULTS

The finite element based on the formulation of previous sections is employed in the static analysis of rectangular plates. The effect of boundary conditions, laminations, and loadings on the bending deflections and stresses is investigated. In the following analyses, two types of materials properties, typical of advanced fiber-reinforced composites, are employed:

Material I: $E_1/E_2 = 25$, $G_{12}/E_2 = 0.5$, $G_{23}/E_2 = 0.2$, $\nu_{12} = 0.25$

Material II: $E_1/E_2 = 40$, $G_{12}/E_2 = 0.6$, $G_{23}/E_2 = 0.5$, $\nu_{12} = 0.25$

It is assumed that $G_{12} = G_{23}$ and $\nu_{12} = \nu_{13}$. A value of 5/6 was used for the shear correction coefficients, $k_1^2 = k_2^2$ (see Whitney [14]). All of the computations were carried out on an IBM 370/158 computer.

First the effect of various boundary conditions on the bending deflection is investigated. Table 1 contains deflections for six types of boundary conditions. BC-I corresponds to a simply supported case, BC-II corresponds to the case in which two vertical sides are simply supported and the other two sides clamped, and BC-III through BC-VI correspond to various clamped cases. Note that there are great differences between the deflections obtained by BC-III and BC-V. The finite element results are in close agreement with the exact solutions of Timoshenko [15] and Das and Rath [16]. Table 2 contains bending deflections for BC-I and BC-II for isotropic ($\nu = 0.3$) plate subjected to uniform temperature distribution (i.e., $q = 0$, $P_1 = 0$, $P_2 = 0$, $T_o = 0$, $\bar{T}_1 = 1.0$). The finite element results are in good agreement with Timoshenko [15] for all aspect ratios. The table also shows the numerical convergence of linear and quadratic finite elements.

Figures 1a and 1b show variation of the bending deflection with the aspect ratio, and side-to-thickness ratio for isotropic and orthotropic single-layer plates. Note that the deflection increases with decreasing aspect ratio for thin isotropic plates, whereas for orthotropic plates (Material I, $\alpha_2 = 3\alpha_1$), the deflection increases slowly with $a/b > 1$ and then decreases. That is, orthotropic materials have a damping effect on the transverse deflection. The effect of thickness shear strain on the deflection is shown in Fig. 1b. for different aspect ratios of single-layer orthotropic plate. It is clear that there is less than 10% increase in deflection for thick plates (compared to the thin plate deflection) subjected to thermal loading, whereas it is known that the increase in deflection is of order 30% in plates subjected to mechanical loading. Again, the finite element results are in close agreement with the closed-form solution presented herein.

Table 1. Effect of boundary conditions on the deflection for isotropic plate subjected to uniform temperature ($q=0$, $T_0=0$, $\nu=0.3$)

Mesh	a/b	Deflection, $\bar{w}$		Boundary Conditions
		Exact	FEM	
	1.0	0.9578*	0.9575	
Q4	1.5	0.5824	0.5822	BC-I: $u=w=\psi_x=0$ on CD; $v=w=\psi_y=0$ on BC
	2.0	0.3702	0.3701	
	1.0	0.206+	0.2063	
Q4	1.5	0.036	0.03601	BC-II: $u=v=w=\psi_x=\psi_y=0$ on CD; $v=w=\psi_y=0$ on BC
	2.0	0.0055	0.00561	
	1.0	—	0.0137	
Q4	1.4	—	0.0224	BC-III: $u=v=w=\psi_x=\psi_y=0$ on CD and BC
	2.0	—	0.0276	
	1.0	0.0138*	0.0138	
Q4	1.4	0.0226	0.0226	BC-IV: $u=v=w=\psi_y=0$ on CD; $u=v=w=\psi_x=0$ on BC
	2.0	0.0277	0.0277	
L4	1.0	—	0.0445	BC-V: $u=v=w=\psi_x=0$ on CD; $u=v=w=\psi_y=0$ on BC
	1.2	—	0.0619	
L4	1.0	—	0.0455	BC-IV: $u=v=w=0$ on CD and BC

* Timoshenko [15], + Das and Rath [16]; $\bar{w} = \frac{10t}{\alpha \bar{T}_1 a^2} w$, $\bar{T}_1 = \bar{T}_1^{11}$

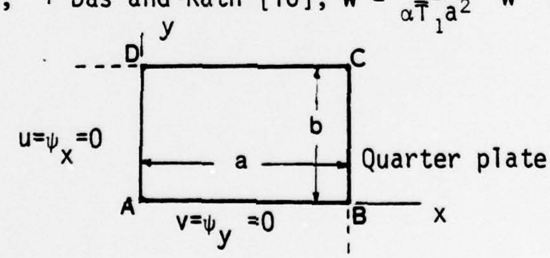

Q4 = 4x4 mesh of (8-node) quadratic elements

L4 = 4x4 mesh of linear elements

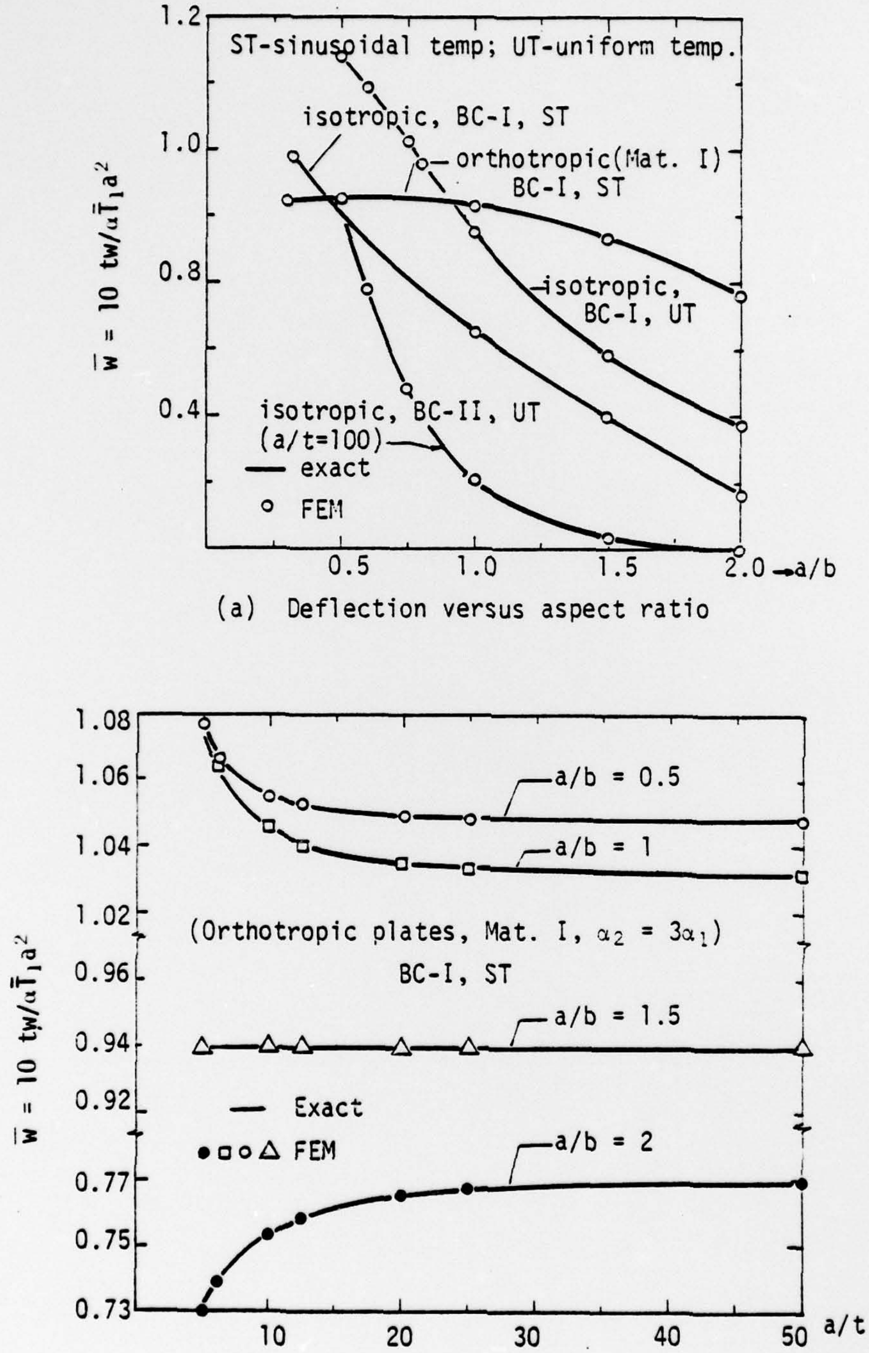

(a) Deflection versus aspect ratio

(b) Deflection versus side-to-thickness ratio

Figure 1. Effects of aspect ratio, side-to-thickness ratio, loading and boundary conditions on the single-layer plates.

Table 2. Effects of the aspect ratio, and side-to-thickness ratio on the deflection+ for isotropic plate subjected to uniform temperature ($q = 0$, $T_0 = 0$, $\nu = 0.3$)

t/a	Source		BC I			BC II		
			a/b=1	a/b=1.5	a/b=2	a/b=1	a/b=1.5	a/b=2
0.01	Das and Rath [16]		0.957*	0.582*	0.370*	0.206*	0.036*	0.0055*
	Timoshenko [15]		0.9578	0.5824	0.3702			
	FEM	L2	1.0833	0.6540	0.4078	0.1927		
		L4	0.9832	0.5965	0.3775	0.2057		
		Q2	0.9632	0.5908	0.3806	0.2005		
		Q4	0.9575	0.5822	0.3701	0.2063	0.0360	0.00561
0.05	Das and Rath [16]		0.960	0.584	0.371	0.213	0.039	0.0067
	Timoshenko [15]		0.9578	0.5824	0.3702			
	FEM	L2	1.0833	0.6540	0.4078	0.2168	0.0127	
		L4	0.9832	0.5965	0.3775	0.2144	0.0332	
		Q2	0.9552	0.5820	0.3710	0.2130	0.0420	
		Q4	0.9576	0.5821	0.3700	0.2132	0.0390	0.0066
0.075	Das and Rath [16]		0.962	0.586	0.373	0.223	0.044	0.0085
	Timoshenko [15]		0.9578	0.5824	0.3702			
	FEM	L2	1.0833	0.6540	0.4078	0.2353	0.0231	
		L4	0.9832	0.5965	0.3775	0.2239	0.0380	
		Q2	0.9554	0.5815	0.3702	0.2210	0.0441	
		Q4	0.9576	0.5821	0.3700	0.2219	0.0432	0.0085
0.10	Das and Rath [16]		0.967	0.589	0.375	0.235	0.050	0.0114
	Timoshenko [15]		0.9578	0.5824	0.3702			
	FEM	L2	1.0833	0.6540	0.4078	0.2545	0.0342	
		L4	0.9832	0.5965	0.3775	0.2363	0.0445	
		Q2	0.9555	0.5813	0.3699	0.2322	0.0491	0.0113
		Q4	0.9576	0.5821	0.3700	0.2330	0.0492	0.0108

* limiting solution as $t/a \to 0$

\+ $\bar{w} = \dfrac{10t}{\alpha \bar{T}_1 a^2} w$

Figure 2 shows the mechanical response of two-layer cross-ply (0°/90°) square plates (Material I) subjected to sinusoidally and uniformly distributed loading ($T_0 = T_1 = 0$). Note that the shear deformation effect is relatively more pronounced for sinusoidal loading than for uniform loading. In Table 3, the deflections due to thermal loading and combined loading are compared with the corresponding closed-form results. The table also contains deflections for single-layer and three-layer (0°/90°/0°) plates. It was noted that the deflections obtained for four-layer, symmetric cross-ply plates (0°/90°/90°/0°) are very close to those obtained for single-layer plates (for the same total thickness).

The effect of thickness and aspect ratio on the thermal and mechanical response of cross-ply plates (0°/90°, 0°/90°/0°, 0°/90°/90°/0°, Material I, $\bar{T}_1 = 1.0$, $\alpha_2 = 3\alpha_1$, $\alpha_1 = 10^{-6}$, $P_1 = P_2 = 0$) is shown in Figure 3. The finite-element solution is in close agreement with the closed-form solution everywhere except for small values of a/t (i.e. for thick plates). The effect of thickness shear on the deflection is less with the increasing aspect ratio. Clearly, the antisymmetric cross-ply plates (0°/90°) have different response characteristics with respect to the aspect ratio when compared with the symmetric cross-ply plates (0°, 0°/90°/0°, or, 0°/90°/90°/0°).

In Figure 4, the closed-form and finite-element solutions of four-layer, cross-ply (0°/90°/90°/0°) plates subjected to sinusoidal temperature distribution and/or mechanical loading are compared. It also contains finite-element solutions for simply supported platessubjected to uniform temperature distribution, and clamped platessubjected to parabolic temperature distribution along y-axis and constant along x-axis. No closed-form solutions are available for these two problems. Specifically, the figure shows non-dimensional deflection versus side-to-thickness ratio for the

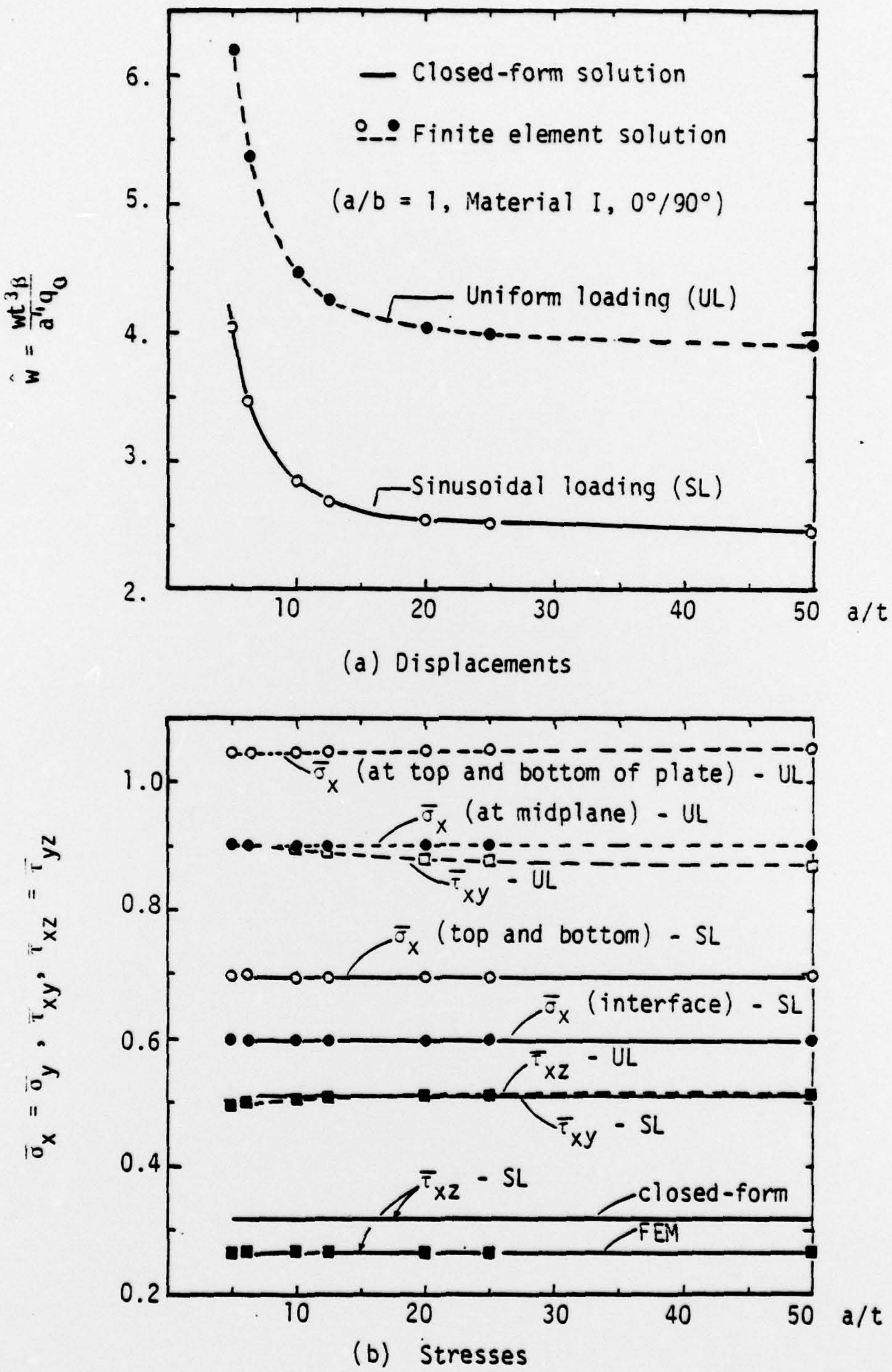

Figure 2 Mechanical bending of two-layer (0°/90°) square plates (Material I).

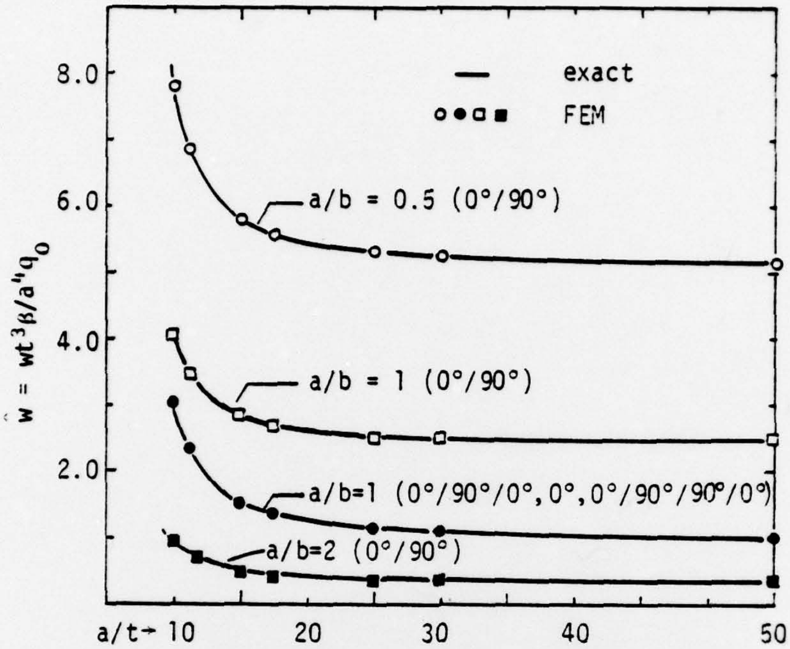

(a) Deflection versus side-to-thickness ratio

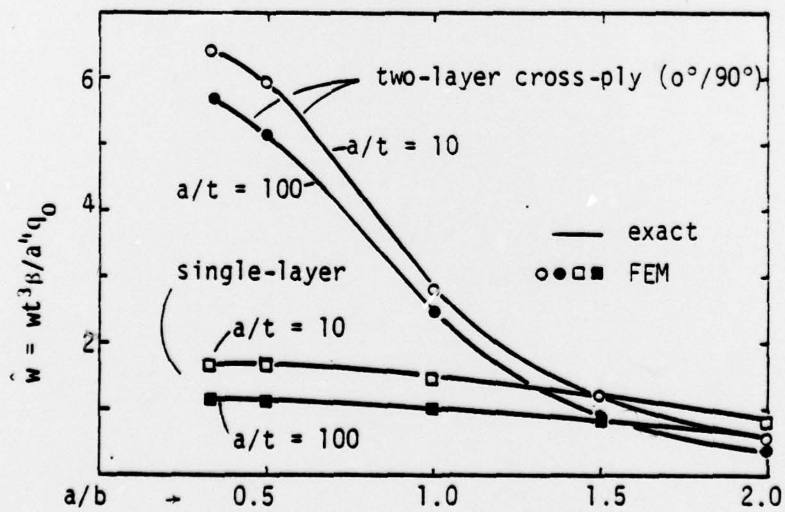

(b) Deflection versus aspect ratio

Figure 3 Effect of thickness and aspect ratio on the deflection of cross-ply plates under combined loading (Material I, $\bar{T}_1$ = 1.0, T_0 = 0, $\alpha_2 = 3\alpha_1$, $\alpha_1 = 10^{-6}$)

Table 3. Effects of loading, lamination, and thickness on the non-dimensionalized deflections for simply-supported (BC-I) square plate (Material I, $\alpha_2 = 3\alpha_1$)

a/t	$\bar{w}$ (sinusoidal temp.)			$\hat{w}$ (sinusoidal temp. and loading)		
	0°	0°/90°	0°/90°/0°	0°	0°/90°	0°/90°/0°
100	1.0313+	1.6765	1.0949	1.0008	2.4563	1.0025
	(1.0312)*	(1.6764)	(1.0948)	(1.0006)	(2.456)	(1.0018)
50	1.0317	1.6765	1.0963	1.0117	2.4625	1.0150
	(1.0317)	(1.6764)	(1.0962)	(1.0116)	(2.462)	(1.0149)
25	1.0334	1.6765	1.1018	1.06068	2.509	1.0802
	(1.0333)	(1.6764)	(1.1017)	(1.0657)	(1.509)	(1.0800)
20	1.0346	1.6765	1.1058	1.1117	2.5448	1.1292
	(1.0345)	(1.6764)	(1.1057)	(1.1116)	(2.544)	(1.1290)
12.5	1.0396	1.6765	1.1224	1.2974	2.7003	1.3372
	(1.0395)	(1.6764)	(1.1223)	(1.2973)	(2.700)	(1.3371)
	1.0440	1.6765	1.1365	1.4672	2.8440	1.5233
10	(1.0439)	(1.6764)	(1.1364)	(1.4670)	(2.844)	(1.5231)
6.25	1.0602	1.6765	1.1870	2.1869	3.4667	2.2832
	(1.0601)	(1.6764)	(1.1869)	(2.1867)	(3.466)	(2.2829)
5	1.0721	1.6765	1.2224	2.8332	4.0416	2.9424
	(1.0720)	(1.6764)	(1.2224)	2.8329)	(4.041)	(2.9421)

+closed-form solution; *finite-element solution

$$\bar{w} = 10\ hw/\alpha_1 \bar{T}_1 a^2\ ,\quad \hat{w} = w\left(\frac{t}{a}\right)^3 \frac{\beta}{q_o a}\ ,\quad \beta = \pi^4\left[4G_{12} + \frac{E_1 + (1+\nu_{12})E}{1-\nu_{12}\nu_{21}}\right]/12$$

following cases(obtained using 2x2 mesh of quadratic elements):

1. simply-supported square plate (SS) subjected to sinusoidal loading (SL) (Material I, $T_o = T_1 = 0$, $P_1 = P_2 = 0$) -○-
2. same as Case 1, except Material II, and sinusoidal temperature (ST) distribution ($\bar{T}_1 = 1.0$) -●-
3. same as Case 1, except sinusoidal temperature (ST) distribution ($\bar{T}_1 = 10^2$) -□-
4. same as Case 1, except $q_o = 0$, and sinusoidal temperature (ST) distribution -■-
5. same as Case 1, except $q_o = 0$, and uniform temperature (UT) distribution ---
6. clamped square plate (CC) subjected to parabolic temperature distribution, equivalent to the mechanical loading, $P_1 = P_2 = 0$, $q = P^*$, where -·-

$$P^* = \frac{E_1(\alpha_1 + \nu_{21}\alpha_2)}{6(1-\nu_{12}\nu_{21})}\bar{T}_1$$

Different nondimensionalizations are used for pure mechanical loading ($\bar{w} = \frac{10^3 w E_2 t^3}{q_o a^4}$) and pure temperature loading ($\bar{w} = \frac{10wt}{\alpha_1 \bar{T}_1 a^2}$). In the case of combined loading, the same nondimensionalization as that in mechanical loading is used. It is found that the thermal bending ($q_o = 0$) is virtually independent of the mechanical properties (i.e. same for Materials I and II) of the plate. Also, the thermal bending ($\bar{w}$) is almost independent of the thickness for sinusoidal temperature distribution. However, it is clear from Case 6 that the thickness effect is more pronounced on the deflection of a clamped plate under parabolic temperature distribution.

Figure 5 shows the effect of thickness on the thermal bending ($q_o = 0$, $P_1 = P_2 = 0$) of cross-ply and angle-ply plates. First note that the deflection scale is amplified (compared to Figure 4) in order to show the relative

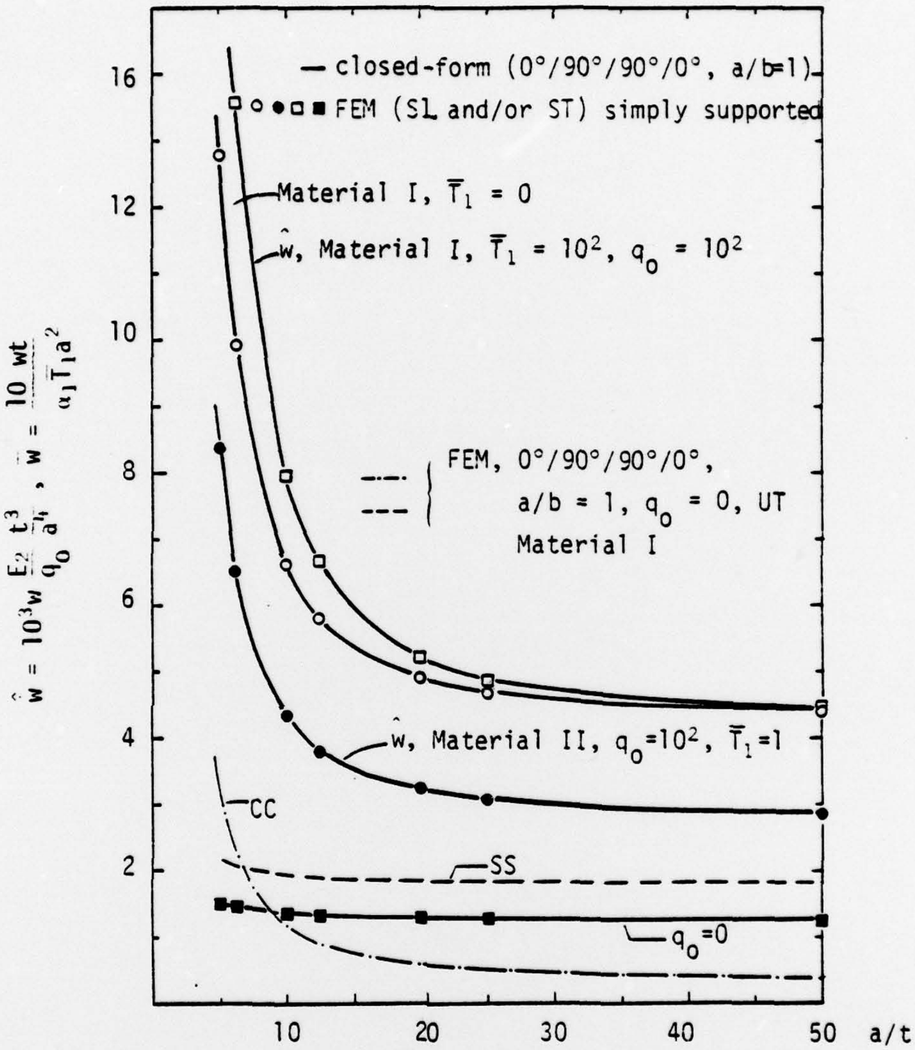

Figure 4 Comparison of closed-form solutions and finite element solutions for four-layer cross-ply (0°/90°/90°/0°) plate.

effect of thickness shear strain. For example, if the deflection for 4-layer (0°/90°/90°/0°) cross-ply (Material II) shown in Figure 5a were plotted to the same scale as that used in Figure 4, it would have overlapped on that shown (in Figure 4) for 4-layer (0°/90°/90°/0°), cross-ply (Material I). Although not plotted, the deflection vs. side-to-thickness ratio plot for the four-layer antisymmetric cross-ply (0°/90°/0°/90°), Material II, a/b = 1) plate is almost identical to that shown for the 4-layer, antisymmetric angle-ply (45°/-45°/45°/-45°, Material II, a/b = 1) except for an additive constant (i.e. shift) of unity (with respect to the nondimensionalization used there). From Figure 5a it is clear that the thickness shear effect is amplified for larger aspect ratios (a/b). Figure 5b shows the normal shear stresses for the two cases for which deflections are plotted in Figure 5a. The thermal bending (deflection as well as stresses) for symmetric angle-ply (45°/-45°/-45°/45°, Material II, a/b = 1) plate was found to be (not shown here for brevity) similar to that of the antisymmetric angle-ply plates for the same material properties, loading, and boundary conditions, except for a small positive shift in the deflection.

SUMMARY AND CONCLUSIONS

A finite-element formulation of equations governing layered anisotropic composite plates subjected to mechanical as well as thermal loading is presented. The element includes the effect of shear deformation and involves five degrees of freedom (three deflections, and two slope functions) per node. Numerical convergence of linear and quadratic elements is shown, and results are presented for cross-ply and angle-ply rectangular plates subjected to sinusoidal and uniform loadings; thermal, mechanical, and combined loadings are considered. To check the finite element results, a closed-form solution is developed herein for cross-ply rectangular plates subjected

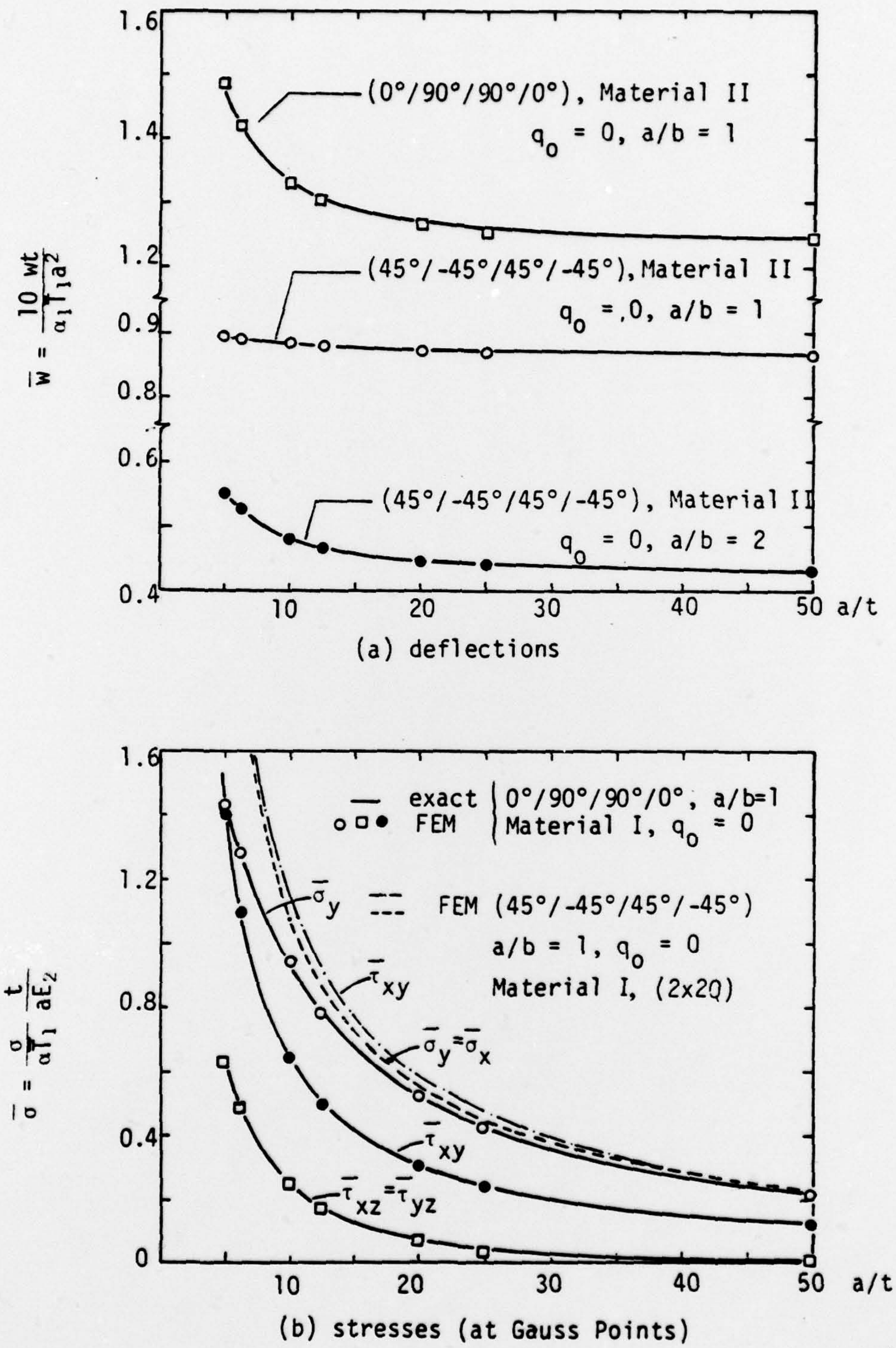

Figure 5 Effect of thickness on the thermal response of cross-ply and angle-ply simply supported plates

to sinusoidal mechanical and/or thermal loadings. The finite-element results agree very well with the closed-form solutions. The maximum error (about 10%) in deflections and stresses occur in the thick plate region (i.e., for side-to-thickness ratios smaller than 10). Thus, the finite element developed herein is computationally simple compared to other plate and shell elements used previously in the thermal stress analysis of plates. Extension of the present element to nonlinear analysis seems to be the next logical step. In that case, the present element saves substantial computational costs.

Acknowledgement The results presented herein were obtained during an investigation supported by the Structural Mechanics Program, Office of Naval Research, Arlington, Va. The authors wish to thank their colleague, Professor C. W. Bert for many helpful discussions.

REFERENCES

1. W. H. Pell, Thermal Deflections of Anisotropic Thin Plates, Q. Appl. Math., Vol. 4, pp. 27-44, 1946.

2. Y. Stavsky, Thermoelasticity of Heterogeneous Aeolotropic Plates, J. Engng. Mech. Div., Proc. ASCE, EM2, pp. 89-105, 1963.

3. N. J. Pagano, Exact Solutions for Rectangular Bidirectional Composites and Sandwich Plates, J. Composite Materials, Vol. 4, pp. 20-24, 1970.

4. P. C. Yang, C. H. Norris, and Y. Stavsky, Elastic Wave Propagation in Heterogeneous Plates, Int. J. Solids and Structures, Vol. 2, pp. 665-684, 1966.

5. J. N. Reddy, Simple Finite Elements with Relaxed Continuity for Nonlinear Analysis of Plates, in Finite Element Methods in Engineering (edited by A. P. Kabaila and V. A. Pulmano), The University of New South Wales, Sydney, Australia, pp. 265-281, 1979.

6. J. N. Reddy, A Penalty Plate-Bending Element for the Analysis of Laminated Anisotropic Composite Plates, Int. J. Numer. Meth. Engng., to appear.

7. C. W. Pryor, Jr. and R. M. Barker, A Finite Element Analysis Including Transverse Shear Effects for Applications to Laminated Plates, AIAA J., Vol. 9, pp. 912-917, 1971.

8. A. S. Mawenya and J. D. Davies, Finite Element Bending Analysis of Multilayer Plates, Int. J. Numer. Meth. Engng., Vol. 8, pp. 215-225, 1974.

9. A. K. Noor and M. D. Mathers, Anisotropy and Shear Deformation in Laminated Composite Plates, AIAA J., Vol. 14, pp. 282-285, 1976.

10. S. C. Panda and R. Natarajan, Finite Element Analysis of Laminated Composite Plates, Int. J. Numer. Meth. Engng., Vol. 14, pp. 69-79, 1979.

11. O. C. Zienkiewicz, R. L. Taylor, and J. M. Too, Reduced Integration Technique in General Analysis of Plates and Shells, Int. J. Numer. Meth. Engng., Vol. 3, pp. 575-586, 1971.

12. T. J. R. Hughes, M. Cohen, and M. Haroun, Reduced and Selective Integration Techniques in the Finite Element Analysis of Plates, Nuclear Engng. & Design, Vol. 46, No. 1, pp. 203-222, 1978.

13. J. N. Reddy, A Comparison of Closed-Form and Finite Element Solutions of Thick Laminated Anisotropic Rectangular Plates (with a study of the effect of reduced integration on the accuracy), Report OU-AMNE-79-18, December 1979, School of Aerospace, Mechanical and Nuclear Engineering, University of Oklahoma, Norman, OK.

14. J. M. Whitney, Stress Analysis of Thick Laminated Composite and Sandwich Plates, J. Composite Materials, Vol. 6, pp. 426-440, 1972.

15. S. Timoshenko, and S. Woinowsky-Krieger, Theory of Plates and Shells, 2nd ed., McGraw-Hill, New York, 1959.

16. Y. C. Das and B. K. Rath, Thermal Bending of Moderately Thick Rectangular Plate, AIAA J., Vol. 10, No. 10, pp. 1349-1351, 1972.

PREVIOUS REPORTS ON THIS CONTRACT

Tech. Rept. No.	OU-AMNE Rept. No.	Title of Report	Author(s)
1	79-7	Mathematical Modeling and Micromechanics of Fiber-Reinforced Bimodulus Composite Materials	C.W. Bert
2	79-8	Analyses of Plates Constructed of Fiber-Reinforced Bimodulus Materials	J.N. Reddy and C.W. Bert
3	79-9	Finite-Element Analyses of Laminated-Composite-Material Plates	J.N. Reddy
4A	79-10A	Analyses of Laminated Bimodulus Composite Material Plates	C.W. Bert
5	79-11	Recent Research in Composite and Sandwich Plate Dynamics	C.W. Bert
6	79-14	A Penalty-Plate Bending Element for the Analysis of Laminated Anisotropic Composite Plates	J.N. Reddy
7	79-18	Finite-Element Analysis of Laminated Bimodulus Composite-Material Plates	J.N. Reddy and W.C. Chao
8	79-19	A Comparison of Closed-Form and Finite-Element Solutions of Thick, Anisotropic, Rectangular Plates	J. N. Reddy

UNCLASSIFIED

SECURITY CLASSIFICATION OF THIS PAGE (When Data Entered)

REPORT DOCUMENTATION PAGE		READ INSTRUCTIONS BEFORE COMPLETING FORM
1. REPORT NUMBER OU-AMNE-79-20	2. GOVT ACCESSION NO.	3. RECIPIENT'S CATALOG NUMBER
4. TITLE (and Subtitle) EFFECTS OF SHEAR DEFORMATION AND ANISOTROPY ON THE THERMAL BENDING OF LAYERED COMPOSITE PLATES		5. TYPE OF REPORT & PERIOD COVERED Technical Report No. 9
		6. PERFORMING ORG. REPORT NUMBER
7. AUTHOR(s) J. N. Reddy and Y. S. Hsu		8. CONTRACT OR GRANT NUMBER(s) N00014-78-C-0647
9. PERFORMING ORGANIZATION NAME AND ADDRESS School of Aerospace, Mechanical and Nuclear Engrg. University of Oklahoma Norman, Oklahoma 73019		10. PROGRAM ELEMENT, PROJECT, TASK AREA & WORK UNIT NUMBERS NR 064-609
11. CONTROLLING OFFICE NAME AND ADDRESS Department of the Navy, Office of Naval Research Structural Mechanics Program (Code 474) Arlington, Virginia 22217		12. REPORT DATE December 1979
		13. NUMBER OF PAGES 25
14. MONITORING AGENCY NAME & ADDRESS (if different from Controlling Office)		15. SECURITY CLASS. (of this report) Unclassified
		15a. DECLASSIFICATION/DOWNGRADING SCHEDULE

16. DISTRIBUTION STATEMENT (of this Report)

This document has been approved for public release and sale; distribution unlimited.

17. DISTRIBUTION STATEMENT (of the abstract entered in Block 20, if different from Report)

18. SUPPLEMENTARY NOTES

19. KEY WORDS (Continue on reverse side if necessary and identify by block number)

Closed-form solutions, composite materials, finite-element solutions, laminated plates, rectangular plates, thermal bending, thermal stresses.

20. ABSTRACT (Continue on reverse side if necessary and identify by block number)

A finite-element formulation of equations governing layered anisotropic composite plates subjected to thermal and mechanical loadings is presented. An exact closed-form solution is also presented for simply supported rectangular cross-ply laminated plates under sinusoidal loading to validate the finite element solutions obtained. The finite element results are in good agreement with the closed-form solutions and with the results of others.

DD FORM 1 JAN 73 1473 EDITION OF 1 NOV 65 IS OBSOLETE
S/N 0102-014-6601

UNCLASSIFIED

SECURITY CLASSIFICATION OF THIS PAGE (When Data Entered)

UNCLASSIFIED

SECURITY CLASSIFICATION OF THIS PAGE(When Data Entered)

UNCLASSIFIED

SECURITY CLASSIFICATION OF THIS PAGE(When Data Entered)